

# Correlation of deep ocean noise (0.4–30 Hz) with wind, and the Holu Spectrum—A worldwide constant

Charles S. McCreery and Frederick K. Duennebieer

*School of Ocean and Earth Science and Technology, University of Hawaii, 2525 Correa Road, Honolulu, Hawaii 96822*

George H. Sutton

*Woods Hole Oceanographic Institution, RD2, Box 167C, Stone Ridge, New York 12484*

(Received 8 July 1991, revised 15 July 1992; accepted 2 December 1992)

One year of ambient ocean noise data, 0.4 to 30 Hz, from the Wake Island hydrophone array in the northwestern Pacific are compared to surface wind speeds, 0–14 m/s (0–28 kn). Between 0.4 and 6 Hz, noise levels increase with wind speed at rates of up to 2 dB per m/s until a saturation is reached having a slope of about  $-23$  dB/octave and a level of 75 dB relative to  $1 \mu\text{Pa}/\sqrt{\text{Hz}}$  at 4 Hz. This noise saturation, called the “Holu Spectrum,” likely corresponds to saturation of short-wavelength ocean wind waves. It is probably a worldwide constant. Between 4 and 30 Hz, noise also increases with wind speed at rates of up to 2 dB per m/s, but no saturation level is observed and the slope increases to about 4 dB/octave. This may be acoustic noise from whitecaps. On a hydrophone less than 3 km from Wake, noise between 0.5 and 10 Hz increases with wind speed at a rate up to 2 dB per m/s, but absolute noise levels are significantly higher than levels on the other hydrophones more distant from Wake, and no saturation is apparent. Surf breaking against the shore of the island is the probable source of this noise.

PACS numbers: 43.30.Nb, 43.30.Pc

## INTRODUCTION

The relationship between ambient infrasonic noise in the deep ocean and corresponding wind and wave conditions on the ocean's surface is a subject that has been studied since at least 1950, when Longuet-Higgins published his theory on the origin of microseisms,<sup>1</sup> the large amplitude, 3–10-s period signals commonly observed on land seismic records. That work, based on the theoretical considerations of Miche<sup>2</sup> and subsequently developed by Hasselman,<sup>3</sup> describes how nonlinear interactions between opposing sets of ocean-surface gravity waves of the same frequency produce double-frequency pressure fluctuations in the water column that do not attenuate with depth. Those double-frequency pressure fluctuations couple into the solid earth and propagate onto land where they are observed as microseisms. There was additional research activity on this subject in the 1960s because of the rapid expansion of instrumental seismology and a corresponding increase in interest in the source and mechanisms of microseismic noise.<sup>4–8</sup> Those studies utilized data collected both on land and in the deep ocean to correlate microseismic noise increases with oceanic storms and surf, and to identify Rayleigh waves as a propagation mechanism for this noise in the solid earth. Within the past 20 years there have been many additional studies that further quantify the relationships between ambient deep ocean noise and various environmental conditions including storms, ocean swell, atmospheric turbulence, wind, wind waves, and breaking wind waves.<sup>9–17</sup> However, most investigators would agree that there are still too few high-quality data in the infrasonic band to produce a comprehensive picture of

the different kinds of deep-ocean noise, their sources, mechanisms of propagation, and the environmental conditions under which they are significant. This paper presents a portion of what has been learned by analyzing a unique long-term set of hydrophone and wind data from the deep ocean near Wake Island in the northwestern Pacific. The data presented here mostly pertain to frequencies above 0.4 Hz.

## I. DATA

The Hawaii Institute of Geophysics (HIG) has digitally recorded signals from at least eight of the hydrophones in the 12-element Wake Island hydrophone array (WIHA) (Fig. 1) since September 1982. This array was built in the late 1950s by the U.S. Air Force, and has been used by HIG since the early 1960s. Signals from these hydrophones have been utilized for studies of guided oceanic-lithosphere seismic phases  $P_0$  and  $S_0$ , mantle-refracted  $P$  phases from distant earthquakes and underground nuclear explosions, seismicity within ocean basins, submarine volcanism, ocean noise, and numerous other topics that can be uniquely studied with long-term data from hydroacoustic sensors located in a mid-ocean basin.<sup>18–21</sup> Six elements of WIHA are located on the ocean bottom (5.5-km depth) at the center and vertices of a 40-km pentagon. The other six elements are located in pairs at three sites, and are at a depth of about 0.85 km—the approximate depth of the SOFAR (sound fixing and ranging) or deep sound channel axis. These passive, moving-coil-type hydrophones are cabled directly to Wake Island. Although designed for signals at frequencies

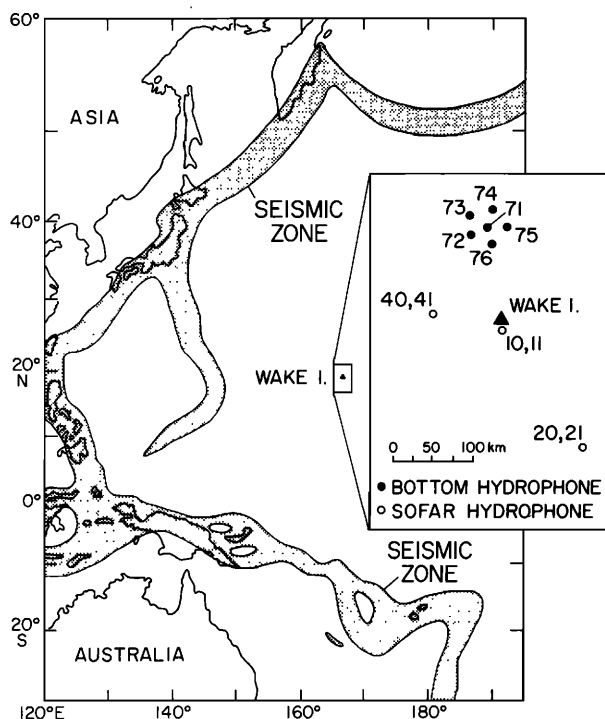


FIG. 1. The position of Wake Island in the northwestern Pacific Ocean, and the relative position of hydrophones in the Wake Island hydrophone array. The hydrophones used in this study are 74, 76, 10, and 20.

greater than 20 Hz, the hydrophones are sensitive to much lower frequencies. Signals with frequencies as low as 0.05 Hz are routinely recorded from moderate to large earthquakes.

The electrical signals generated by the passive hydrophones and transmitted through the long cables must first be amplified by very low-noise preamps. Then, after further amplification, pre-whitening, and anti-alias filtering, the signals are digitized with 16 bits of resolution, multiplexed, and recorded on tape shipped regularly to HIG for analysis. The digitization rate of the data used in this study is 80 Hz. (The digitization rate was increased to 100 Hz in September 1989.) The estimated hydrophone-cable-amplifier-filter-digitizer response curves for the four hydrophones used in this study are shown in Fig. 2. The amplifier-filter-digitizer response was modified for optimal pre-whitening and anti-aliasing during the system installation and was measured in place at Wake Island. The hydrophone response is an estimate extrapolated from data published by Thanos<sup>22</sup> describing the Columbia-Pt. Arena Ocean Bottom Seismic Station (OBSS), an instrument with an identical hydrophone. A small hydrostatic pressure compensation hole in the hydrophone reduces its long-period response by 6 dB/octave below some corner frequency. Thanos put this corner at 3 Hz,<sup>22</sup> although Barstow *et al.*<sup>23</sup> move it to 0.3 Hz based on a comparative analysis of OBSS hydrophone and seismometer data. A 0.3-Hz corner has been assumed for the WIHA hydrophones, although uncertainty about it remains, particularly since the pressure compensation hole may be partially or completely filled after more than 30 yr in the water. The

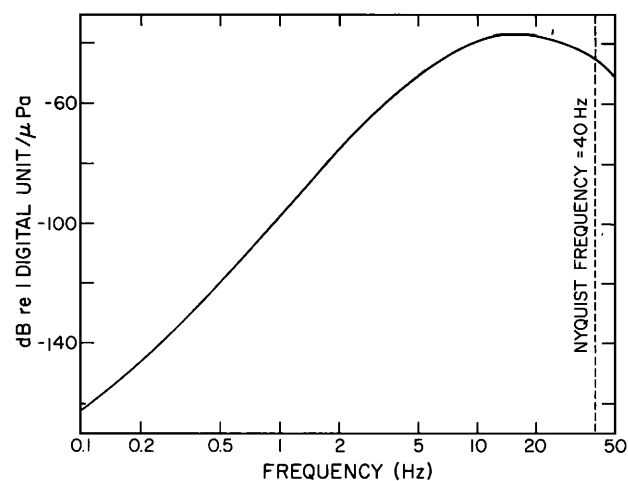


FIG. 2. Estimated response curves for hydrophones 10, 20, 74, and 76 through the recording system of the Wake Island hydrophone array. The general shape of these curves was chosen, by the design of the amplifiers, to whiten the ambient noise between about 0.5 and 20 Hz and to provide anti-aliasing. Notches at 60 Hz are to reduce 60-Hz crosstalk.

cables have an attenuating effect at frequencies greater than about 5 Hz that increases with both frequency and cable length. The depth dependence of the hydrophone response in combination with the different cable lengths lead to four separate response curves for the four hydrophones.

Ambient noise samples, 3 min in length, were extracted from the continuous data at an average rate of one noise sample per hour. The spacing between samples was randomized to minimize the possibility of contamination by electrical noise sources at Wake (such as radio transmissions) which might be on a fixed schedule. A subset of these data, consisting of noise samples from two deep hydrophones, 74 and 76, and two SOFAR hydrophones, 10 and 20, with noise samples spaced approximately every 6 h over the first year of operation is analyzed in this study. The two deep hydrophones are anchored on relatively flat, sediment-covered ocean floor; SOFAR hydrophone 10 is anchored on the submarine flank of Wake Island; and SOFAR hydrophone 20 is suspended above the side of a seamount.

Complementing the ambient noise data are weather data from the National Weather Service (NWS) station at Wake Island. Among the various measurements made by NWS at Wake are wind speed and wind direction, measured every hour with daily averages reported in monthly summaries.<sup>24</sup>

## II. DATA REDUCTION

### A. Spectral computation

The first major step in the analysis of these data was transformation from the time domain to the frequency domain. Each 3-min time series was divided into 27 adjacent 512-point segments that were each demeaned, deskewed, Lanczos-windowed (to approximately preserve absolute amplitudes), and then transformed with a 512-point fast

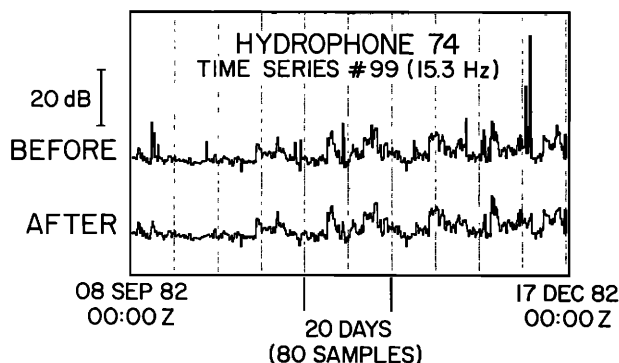


FIG. 3. A sample 100-day time series of ambient noise fluctuations before (upper) and after (lower) the removal of extraneous transient signals.

Fourier transform (FFT). Mean power spectral levels at each of the resulting 256 frequencies were computed by averaging data from the 27 transformed segments. This procedure produces spectral levels with more stability than their constituent spectral estimates, with a sacrifice in frequency resolution relative to that that would be achieved by transforming the entire 3-min time series with one FFT. The hydrophone-cable-recording system responses were then applied to the data to put them into absolute pressure units. Finally, the data were normalized to a 1-Hz bandwidth.

Four large data sets were produced, one for each hydrophone. Each data set consists of 256 time series of spectral noise levels—one for each of the 256 spectral frequencies. Each time series is 1460 samples in length (i.e., 365 days  $\times$  4 samples/day = 1460 samples). These time series represent the ambient noise level fluctuations over a 1-yr period for a particular hydrophone at a particular frequency. Only the first 192 (0 to 30 Hz) of each hydrophone's 256 time series were analyzed further.

### B. Removal of transients

Unwanted high-energy transients were present in each of the time series, and an attempt was made to remove them. Sources for these transients include earthquakes, nearby shipping, and geophysical surveys. A transient was empirically defined as any individual sample with a power level at least 3 dB greater than the level of the two adjacent samples in the time series. Transients were replaced by the mean value of those two adjacent samples. This procedure successfully removed extraneous spikes in the data, while preserving most of the original character of the time series (Fig. 3). At a maximum, only about 10% of the data points of any time series were modified by this procedure (Fig. 4). It is interesting to note that the percent number of transients in a particular time series appears to be directly proportional to the noise frequency that the time series represents, at least for frequencies between 0 and 20 Hz. This is partially a consequence of rapidly decreasing absolute noise levels between 0.2 and 10 Hz.

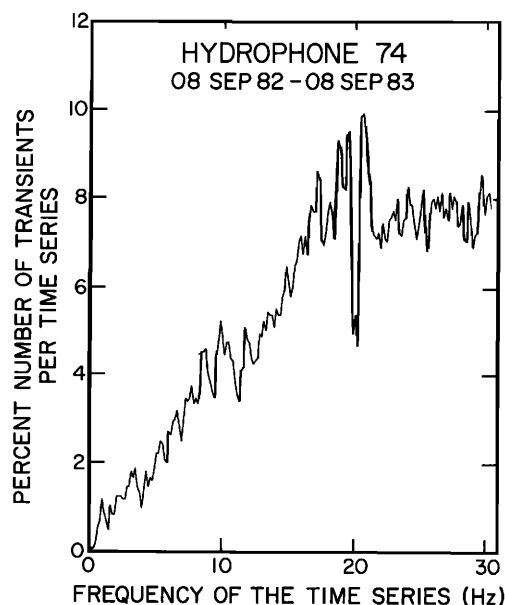


FIG. 4. The percent number of data points considered to be extraneous transients in each time series are plotted as a function of the frequency of the time series. The feature at 20 Hz is an artifact caused by an aliased 60-Hz signal.

### III. ONE-YEAR MEAN NOISE LEVEL SPECTRA

The 1-yr mean noise spectra from the four hydrophones studied exhibit characteristics typical of deep ocean noise spectra (Fig. 5). Levels are highest at the lowest frequencies. The microseism peak is somewhere between 0.1 and 0.3 Hz, although the spectral resolution of this study (0.156 Hz) is too coarse to resolve that peak with any precision. Between 0.3 and 6 Hz, levels fall off rapidly with frequency, and above 10 Hz the spectral slope is flat or slightly positive. A narrow peak at 20 Hz in the spectra of hydrophones 74 and 76 is an artifact (60-Hz energy aliased to 20 Hz). A broader rise in level at about 17 Hz on all hydrophones, however, is caused by whales. Whale signals are easily identified in the time record and similar signals have been described and identified by Urick,<sup>25</sup> Watkins *et al.*,<sup>26</sup> and Northrop *et al.*<sup>27</sup> The standard deviations shown around each curve in the figure should be viewed with some caution since the actual distribution of data points about the mean at any frequency is not Gaussian, as will be demonstrated later.

Differences between the four 1-yr means are shown in Fig. 6, using hydrophone 74 as the reference at 0 dB. The two bottom hydrophones, 74 and 76, have nearly identical means as might be expected from their 40-km spacing and similar environment. Differences between these two curves at frequencies above 10 Hz may be the result of small errors in the estimates of their respective cable responses. Suspended SOFAR hydrophone 20 is quieter than 74 below about 2 Hz, and noisier above 3 Hz. Increased levels at high frequencies are due to this hydrophone's location within the SOFAR channel, a highly efficient waveguide capable of propagating noise at these frequencies over many thousands of kilometers. Levels are consistently lower below about 2 Hz, with the difference increasing to

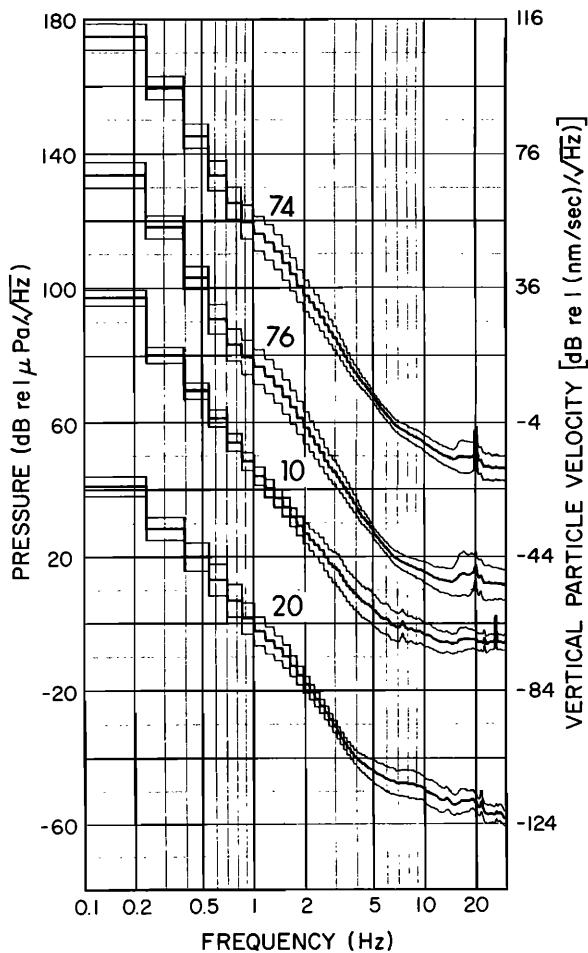


FIG. 5. One-year mean ambient noise level spectra, plus and minus one standard deviation, for hydrophones 74, 76, 10, and 20. Vertical particle velocities corresponding to acoustic pressure fluctuations are computed using the formula: pressure = water density  $\times$  sound velocity in water  $\times$  vertical particle velocity.

18 dB near 0.15 Hz. Although this difference could be nearly eliminated by using a higher frequency pressure compensation corner in the response curve of hydrophone 20, its shallower depth (780 vs 5400 m) could also be the cause of the difference. For example, if the low-frequency noise is predominantly fundamental mode Rayleigh waves, then for a given amplitude of bottom motion the pressure in the water below a certain frequency is proportional to the depth (i.e., the water simply acts as a passive load on the bottom<sup>28</sup>). In this case, the difference in depth would produce a 17-dB difference in level, in good agreement with the above observation. SOFAR hydrophone 10 is generally noisier than all other hydrophones. This is most likely the result of its location only 3 km from the shores of Wake, where breaking surf is an additional energetic source of noise.

The 1-yr mean noise spectra of hydrophones 74 and 20 are compared to several other oceanic and continental ambient noise spectra in Fig. 7. The WIHA curves are most similar to the other oceanic curves, two from hydrophones in the Atlantic<sup>12</sup> and one from a differential pressure gauge in the Pacific.<sup>29</sup> Two continental noise spectra, corrected to

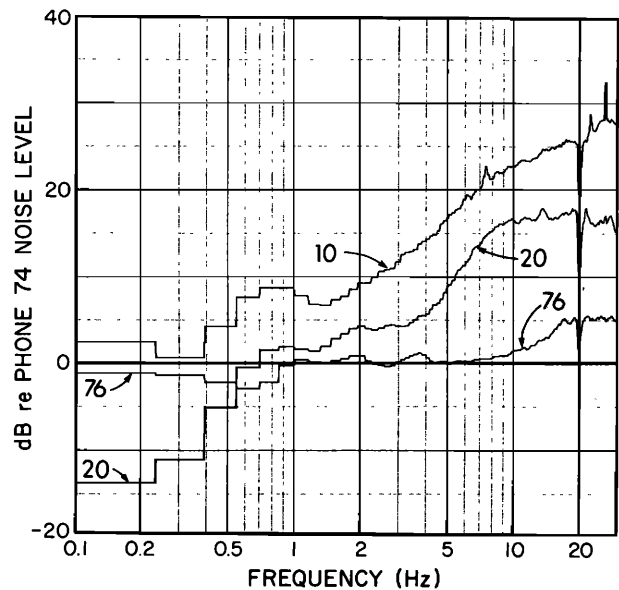


FIG. 6. The one-year noise means of hydrophones 76, 10, and 20 measured relative to the one-year noise mean of hydrophone 74 at 0 dB.

pressure, are also shown for reference. One of them represents the average ambient noise on continents,<sup>30</sup> and the other is from an extremely low noise site in Texas.<sup>31</sup>

#### IV. TEMPORAL VARIATIONS OF THE NOISE AND WIND

In order to graphically view the information contained in the 192 time series associated with each hydrophone, the data were reduced into only 15 time series for each hydrophone. These new time series represent the ambient noise level fluctuations over the 1-yr period in 15 contiguous 2-Hz bands from 0 to 30 Hz. Computation of the new time series was made as follows. Each 2-Hz band represents approximately 13 original time series (i.e., 192 original/15 new = 12.8). Each data point in an original time series represents the noise level for a particular 6-h time period in a 0.156-Hz frequency band (i.e., 30 Hz/192 = 0.156 Hz). By averaging the dB noise levels from the appropriate original time series for each 2-Hz band, 15 new time series are formed. If an original time series was just fractionally represented in a particular 2-Hz band, then it was included in the average only if that fraction was greater than one-half. Note that by averaging in log space (dB), similarities in the shapes of the original time series are emphasized—the original time series with the most power does not unduly influence the result. Similarly, note that in the 0–2 Hz band this type of averaging will de-emphasize the microseism peak data since it is represented only in the two lowest-frequency original time series.

The 15 time series from hydrophone 74 are shown in Fig. 8. The 2–4 Hz time series appears truncated across the top, and exhibits noise lows that are as much as 15 dB below the apparent noise ceiling. Similar features at these frequencies were reported by Duennebieer *et al.*<sup>32</sup> in the ambient noise data from a long-term deployment of HIG's ocean sub-bottom seismometer down a deep-sea drill hole

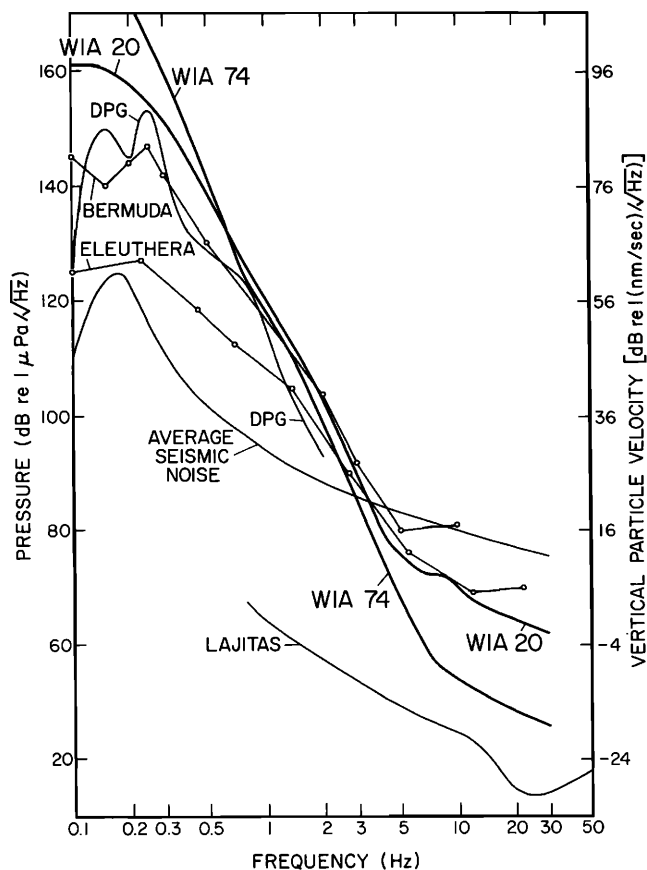


FIG. 7. The one-year mean noise spectra of WIHA hydrophones 74 and 20 compared to noise measurements made elsewhere. The Eleuthera Island measurement is a 6-week average made by Nichols<sup>12</sup> using a hydrophone at 1300-m depth. The Bermuda Island measurement is an average of four 10-min samples taken during 6.4-m/s average winds using a hydrophone at 4300-m depth (Talpey-Worley data reported by Nichols<sup>12</sup>). The differential pressure gauge data (DPG) reported by Cox *et al.*<sup>29</sup> was collected at 1600-m depth off the California coast. The "average seismic noise" reported by Brune and Oliver<sup>30</sup> is from vertical seismometer measurements made on continents. The Lajitas, Texas curve given by Herrin<sup>31</sup> represents very low continental noise.

near the Kuril Islands. The time series for frequencies above 6 Hz, on the other hand, appear truncated at the bottom and exhibit noise peaks with amplitudes 20 dB or more above the apparent noise floor. The 4–6 Hz time series seems to be a transition between the 2–4 and > 6 Hz bands, and is flat-middled with some lows and some peaks. Only the 0–2 Hz curve appears to be unrestricted throughout its amplitude range. Some of the large amplitude signals most prominent on the 16–18 Hz curve but also visible on adjacent curves are caused by whales.

One hundred days of ambient noise in six of the fifteen 2-Hz bands for all four hydrophones is shown in Fig. 9. Curves for the two bottom hydrophones, 74 and 76, appear similar in all bands as might be expected given that these two hydrophones are at the same depth and are only 40 km apart. Comparisons between curves for the bottom and the SOFAR hydrophones show far fewer similarities. They appear perhaps the most coherent in the 0–2 Hz range where absolute noise levels are also the most similar. Above 2 Hz, the SOFAR hydrophones are decreasingly coherent with

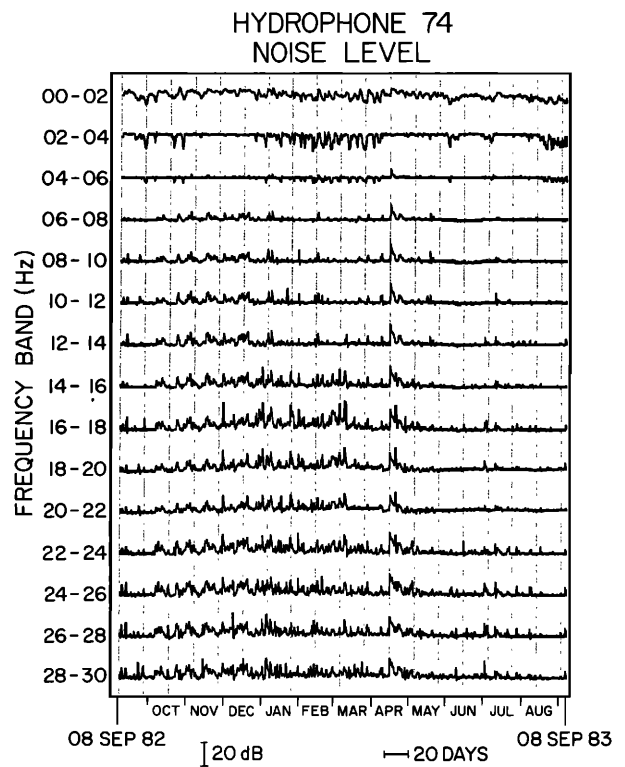


FIG. 8. A plot of the temporal variations in ambient noise over one year for all fifteen 2-Hz bands from Wake bottom hydrophone 74.

respect to the bottom hydrophones and with respect to each other.

The relationship between ambient ocean noise and wind is demonstrated in Fig. 10. It compares six of the 1-yr-long, 2-Hz-wide time series from hydrophone 76 with time series of the Wake daily mean wind speed and direction from the NWS monthly summaries. At 0–2 Hz, the two data sets are remarkably similar, with nearly all major features represented in both curves. At 2–4 Hz and 4–6 Hz, noise lows nearly always correspond with low wind, and above 6 Hz noise peaks nearly always correspond with high wind.

To quantify these similarities, correlation coefficients and lag times were computed between the wind speed curve and each noise curve. Values are given in Table I. The 0–2 Hz noise data have a fairly high correlation coefficient, 0.77, and a lag time of +6 h, indicating that the noise is delayed relative to the wind by an amount equal to one sampling interval. This time shift may be an indication of the lag between the onset of winds and the full development of waves that produce the noise. The correlation coefficient for the 2–4 Hz data is 0.54 with a lag of +6 h. That correlation can be improved to 0.71, with the same lag, by truncating the wind speed curve for values above 6.26 m/s (the mean wind speed) to give it a character more like the 2–4 Hz noise curve. The correlation coefficient for the 4–6 Hz curve is 0.49 with a lag of 0 h. This lower correlation is probably attributable to the relative lack of features in the noise curve for this frequency band. The 12–14 Hz curve has a correlation coefficient of 0.67 with a lag of 0 h. Similar correlation and lag values are

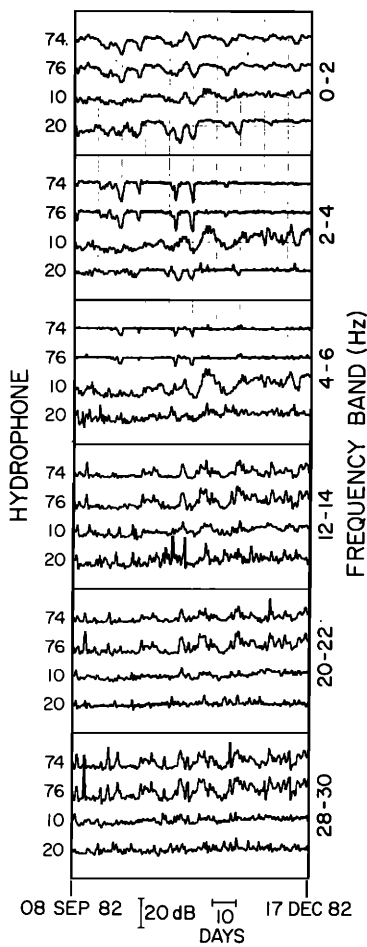


FIG. 9. Comparison in six frequency bands between temporal noise level fluctuations of the four hydrophones studied over a 100-day period.

TABLE I. Correlation coefficients and lag times for the wind speed time series compared to each ambient noise time series. Values shown are the maximum correlation coefficient followed by its corresponding lag in hours. A positive lag indicates that the noise lagged behind the wind.

Frequency band (Hz)	Hydrophone 74	Hydrophone 76	Hydrophone 10	Hydrophone 20
00-02	0.77/+06	0.80/+06	0.80/+06	0.78/+12
02-04	0.54/+06	0.56/+06	0.65/+12	0.38/+12
04-06	0.49/+00	0.57/+00	0.65/+18	0.26/+36
06-08	0.64/+00	0.73/+00	0.62/+18	0.28/+30
08-10	0.65/+00	0.72/+00	0.55/+18	0.26/+30
10-12	0.66/+00	0.73/+00	0.54/+18	0.28/+12
12-14	0.67/+00	0.73/+00	0.47/+24	0.25/+06
14-16	0.57/+00	0.60/+00	0.42/+18	0.22/+06
16-18	0.27/+00	0.31/+00	0.23/+18	0.21/+12
18-20	0.30/+00	0.33/+00	0.25/+30	0.18/-06
20-22	0.34/+00	0.37/+00	0.31/+30	0.22/-06
22-24	0.48/+00	0.48/+00	0.34/+18	0.27/-06
24-26	0.52/+00	0.52/+00	0.40/+12	0.30/+00
26-28	0.54/+00	0.54/+00	0.35/+18	0.27/-06
28-30	0.51/+00	0.51/+00	0.36/+18	0.20/+00

found for all other curves between 6 and 16 Hz. A much lower correlation, 0.34 with a lag of 0 h, was found for the 20-22 Hz data, and low values were also found for 16-18 and 18-20 Hz curves (not shown). These low correlation values are probably the result of partial contamination of the noise data by the aforementioned 20-Hz artifact and whale noises. The correlation coefficient for the 28-30 Hz curve is 0.51 with a lag of 0 h, and similar values were found for the other curves between 22 and 28 Hz. The 0-h lag found for all curves above 4 Hz indicates that noise at these frequencies responds quickly to changes in wind speed. Correlations and lags for hydrophone 76 are very

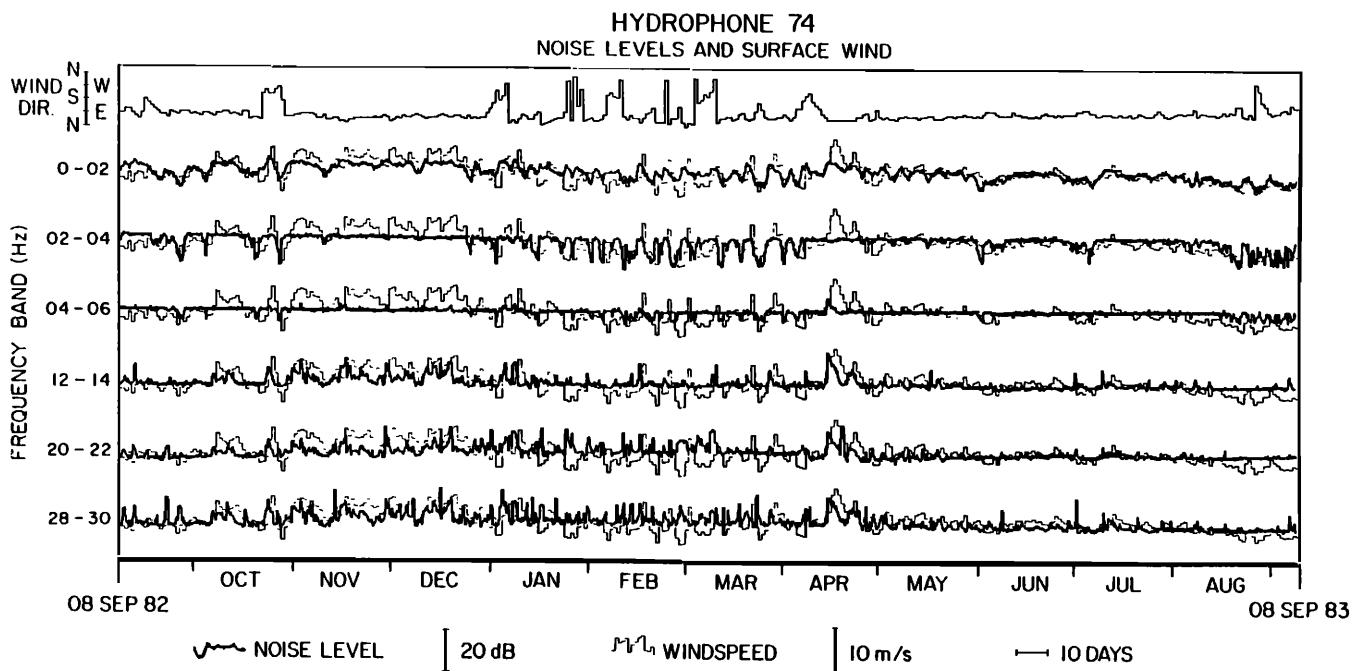


FIG. 10. Comparison between the temporal fluctuations of the ambient ocean noise on hydrophone 74 in six frequency bands (thick lines), the daily mean wind speed at Wake Island (thin lines), and the daily mean wind direction at Wake Island (top).

similar to those for hydrophone 74, as might be expected. Slightly higher correlation values for hydrophone 76 may be because this hydrophone is 40-km closer to Wake Island where the wind speeds are measured.

Hydrophone 10, located just offshore of Wake Island, has a correlation of 0.80 and a lag of +6 h for its 0–2 Hz time series compared to wind speed. The 2–4 Hz time series has a correlation coefficient of 0.65 with a lag of +12 h. These values are similar to those found for the deep bottom hydrophones, although the 2–4 Hz lag is one sample longer. Between 4 and 16 Hz the six correlation coefficients average 0.54, but there are five lags of +18 h and one lag of +24 h. These long lags are consistent with a hypothesis that this noise is from waves breaking on the shoreline of Wake. The longer wavelength ocean waves associated with surf take more time to develop in the wind. Between 16 and 22 Hz, correlations are again much lower, averaging 0.26. Above 22 Hz there is only a slight increase in the average correlation to 0.36. Lag times for these seven curves are also long, averaging more than 20 h.

The correlation coefficients for hydrophone 20 at 0–2 and 2–4 Hz are 0.78 and 0.38, respectively, with lags of +12 h. This somewhat longer lag relative to the other hydrophones could be caused by a combination of hydrophone 20's location more than 150 km to the southeast of Wake and the northwesterly approach of most frontal systems passing Wake. Above 4 Hz, correlation coefficients are uniformly low, averaging 0.25, with lags that vary from –6 h to +30 h. These low correlations are also probably due to hydrophone 20's long distance from Wake, as well as its location at the depth of the SOFAR channel axis. At this depth it is probably receiving noise generated over a broader region of the ocean's surface relative to the region heard by the deep bottom hydrophones whose noise levels above 4 Hz correlated more highly with wind speed. This contention is supported by the data in Fig. 6 showing that hydrophone 20 also has significantly higher absolute noise levels above 4 Hz relative to the bottom hydrophones.

Also shown in Fig. 10 is a time series of the daily mean wind direction at Wake. Kibblewhite and Ewans<sup>11</sup> have noted significantly increased ambient noise levels between 0.1 and 5 Hz measured by land seismometers along the west coast of New Zealand at the time of large shifts in the offshore wind direction, even in a moderate wind field. They attribute this elevated noise to increased pressure fluctuations on the ocean floor which are in turn caused by enhanced nonlinear wave interactions (Longuet-Higgins' theory<sup>1</sup>) due to the wind shift. The Wake data, however, do not seem to exhibit the effect observed by Kibblewhite and Ewans, since there are many large changes in wind direction unaccompanied by corresponding increases in noise.

## V. NOISE SPECTRA VERSUS WIND SPEED

The mean noise spectra for eight wind speed ranges from each of the four hydrophones is shown in Fig. 11. Each individual spectrum was determined by averaging all noise spectra over the 1-yr period from data recorded when the wind speed was within that particular range. The num-

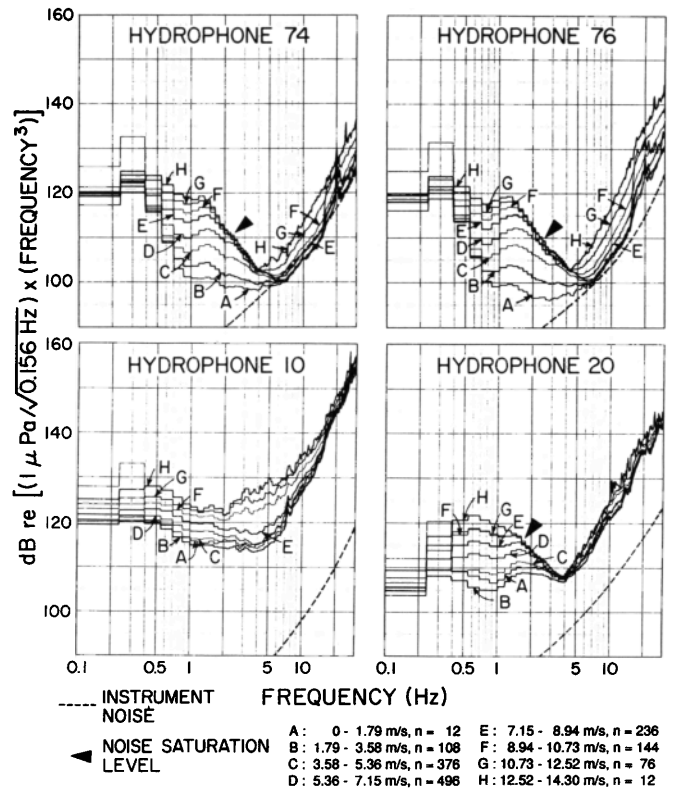


FIG. 11. Noise spectra from each hydrophone averaged in eight wind speed ranges. The number of spectra averaged together in each wind speed group,  $n$ , is indicated in the legend. Estimated instrumental noise levels are indicated by the dashed lines on each plot. The spectral data are multiplied by their frequency in  $\text{Hz}^2$  to aid in visualization.

ber of spectra averaged in each wind speed range is different and is indicated on the plot. The spectral level of each data point, in microPascals ( $\mu\text{Pa}$ ), has been multiplied by its frequency squared before converting it to decibels (dB). This procedure has the effect of “rotating” each spectrum counterclockwise about its value at 1 Hz by 12 dB per octave. This rotation helps to visually clarify differences between individual spectra. Without it, the seven spectra in each plot would be indistinguishably bunched together because of their steep spectral slope. To convert a data point on this plot back to more conventional units of “dB relative to  $1 \mu\text{Pa}/\sqrt{\text{Hz}}$ ” simply add a correction term to its dB value on the plot. This correction term,  $-40 \times \log_{10}(f)$ , where  $f$  is the frequency of the data point in Hz, undoes the rotation. Figures 5 and 7 show similar data in these more conventional units.

The spectra in Fig. 11 from the two deep hydrophones, 74 and 76, are nearly identical. At the lowest frequencies, between 0.1 and 0.2 Hz, there is little variation that correlates with local winds. This is the band that contains the prominent worldwide spectral peak of double-frequency storm microseisms. The low correlation is not surprising since winds less than 14 m/s, the highest found in these data, are not expected to efficiently generate the 0.05 to 0.1 Hz swell required.<sup>33</sup> However, the observed variation in this band is large (20 to 30 dB) and is probably produced by Rayleigh waves generated near Wake by the interaction

of storm swell and its reflection from the Wake platform, or Rayleigh waves propagating from more distant sources. Sutton and Barstow<sup>15</sup> present a clear demonstration of Rayleigh wave generation near an ocean-bottom seismometer by swell from distant storm centers. Further investigations of this frequency band, using spectra of higher resolution, are in progress.

Between 0.4 and 6 Hz, noise levels increase regularly with wind speed at rates of up to 2 dB per m/s until a saturation is reached, above which levels do not rise. This saturation is clearly apparent between about 1.5 and 5 Hz with a slope of about  $-23$  dB/octave ( $-11$  dB/octave on the rotated plot) and an absolute level of about 75 dB (99 dB on the rotated plot) at 4 Hz. It occurs at the highest frequencies when winds are low, but migrates to lower frequencies as winds increase. The saturation is not instrumental, since transient signals commonly exceed these levels by tens of dB. Between 0.3 and 0.8 Hz, the noise is bounded from below by minimum levels having a slope of about  $-30$  dB/octave ( $-18$  dB/octave on the plot). This feature does not appear related to the wind speed and it may be the high-frequency flank of the microseism peak. It is being investigated further. Between 6 and 30 Hz, low wind speed levels are close to the estimated system noise (dashed line). When the wind speed exceeds about 8 m/s, noise levels increase at rates of up to 2 dB per m/s. The spectral slope of this noise increases with frequency to about  $+4$  dB/octave ( $+16$  dB/octave in the figure) for frequencies  $> 10$  Hz. Between 4 and 6 Hz this type of noise sometimes rises above the aforementioned saturated noise.

The phenomenon generating noise between 0.4 and 6 Hz is most likely local wind waves. If a 2:1 relationship between noise and wave frequencies is assumed, as predicted by nonlinear wave interaction theory, then the waves responsible for this noise have frequencies between 0.2 and 3 Hz. Phillips<sup>34</sup> has compiled data showing that ocean waves at these frequencies also exhibit a saturation or equilibrium above which they do not grow. Ocean waves with frequencies above 1.5 Hz have wavelengths less than 0.7 m and phase velocities less than 1 m/s. Such waves should reach equilibrium often in the winds common to Wake, and as a consequence, the ocean noise above 3 Hz near Wake should also be frequently saturated. From the figure it appears such saturation occurs about half the time. It is likely that deep ocean noise worldwide is also commonly saturated in this band. McCreery and Duennebieer have named this saturated ocean noise the "Holu Spectrum," from the Hawaiian word for deep ocean.<sup>35</sup> Not only is the slope of the Holu Spectrum constant, its absolute level appears to have little if any variation with depth in the water column (note that levels on SOFAR hydrophone 20 are similar to those on the deep hydrophones), implying that it can be used as a constant for *in situ* calibration of ocean seismoacoustic instrumentation. In addition, noise levels in this band may yield a direct estimate of the ocean wave spectrum at short wavelengths.

At frequencies above 4 Hz, deep ocean noise may be acoustic signals from whitecaps or open-ocean breaking waves. This mechanism was proposed by Duennebieer

*et al.*<sup>36</sup> based on data from a deep sea borehole seismometer. Like the WIHA deep hydrophones, the borehole seismometer exhibited noise levels that only began to rise when winds exceeded a certain speed. This characteristic is suggestive of whitecaps, since they too begin to form only when winds are above a certain speed. The Beaufort scale puts the whitecap wind speed threshold at 4 m/s, although Wake noise levels do not begin to increase until wind speeds exceed about 8 m/s. Measurements of this type of noise on WIHA hydrophones in the extreme winds of a typhoon show that it grows without bounds. These typhoon noise data will be presented in a later report.

The spectral view of the noise (Fig. 11) complements the time series view (Figs. 8, 9, and 10) discussed earlier. The flat top of the 2–4 Hz time series is the spectral saturation level; the flat middle of the 4–6 Hz time series is also the saturation level, sometimes overridden at high wind speeds by the higher frequency noise mechanism; and the flat bottoms of the time series above 6 Hz reflect the spectral noise minimum in this frequency band. Only the 0–2 Hz time series has a relatively unrestricted range, as do most of the spectral data in that band. In this band the noise is seldom saturated, thus reflecting a continuous variation with wind speed.

The noise spectra of suspended SOFAR hydrophone 20, also shown in Fig. 11, are very similar to those of the bottom hydrophones. Levels regularly increase with wind speed between 0.4 and 4 Hz at rates of up to 2 dB per m/s. Saturation of the noise is clearly visible between 1.5 and 4 Hz with a slope of about  $-20$  dB/octave ( $-8$  dB/octave on the plot), only slightly less steep than that observed on the deep hydrophones. This slight difference could be due to calibration errors. Absolute levels of the Holu Spectrum on this SOFAR hydrophone are very close to those found on the deep bottom. Above 4 Hz there is again a sharp difference in spectral slope to  $+3$  dB/octave ( $+15$  dB/octave on the plot) at frequencies  $> 10$  Hz; however, noise levels increase with wind speed at rates less than 0.4 dB per m/s (this relation is not easily seen in the figure due to the closeness of the curves). The reduced rate of these increases with wind speed and the higher absolute amplitudes relative to those observed on the deep bottom hydrophones may be caused by this hydrophone's location at the depth of the SOFAR channel axis, and thus its susceptibility to high-frequency noise from more distant sources. Instrumental noise is not a factor in these spectra.

The spectra from SOFAR hydrophone 10 are also clearly wind related, although they have a much different character than those of the other three hydrophones. Over the entire band shown in the figure, 0.1 to 30 Hz, noise levels grow with increasing wind speed. The highest rates of growth, up to 2 dB per m/s, are found between about 2 and 6 Hz. There is no saturation level apparent in these spectra, nor is there an abrupt change in spectral slope at around 4 Hz, but only a more gradual change between 1 and 10 Hz. In addition, as noted previously, absolute noise levels are generally higher than those observed on the other three hydrophones. These differences are probably the result of hydrophone 10's close proximity to Wake Island,

## HYDROPHONE 74

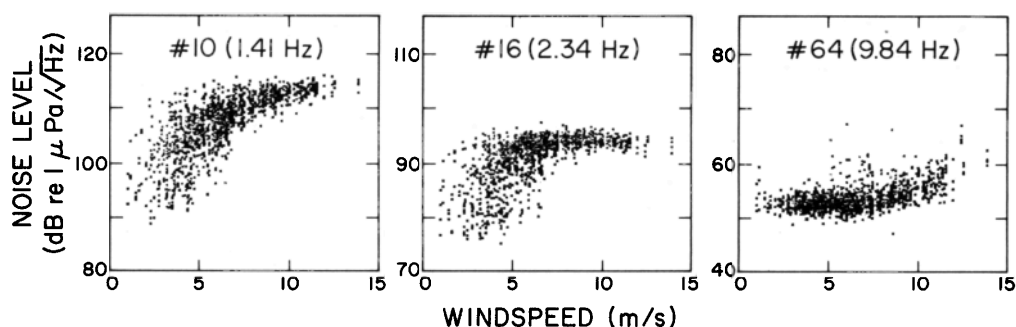


FIG. 12. Each of the 1460 noise level measurements from hydrophone 74 made over a 1-yr period at three discrete frequencies, plotted as a function of wind speed to show the level of scatter in the data. The spectral estimate number and its corresponding frequency are noted for each plot.

where additional noise is generated by the breaking of wind waves and swell on the shore of the island.

### VI. NOISE LEVEL VERSUS WIND SPEED SCATTER

The distribution of the 1460 individual noise level measurements from hydrophone 74, were examined at three discrete frequencies out of the possible 192 as a function of wind speed (Fig. 12). The largest range of noise levels is at 1.41 Hz, although the saturation level is clearly visible. Scatter at this frequency varies from about 20 dB at the lower wind speeds to less than 5 dB at the higher wind speeds where the noise is saturated. At 2.34 Hz the saturation level is dominant over a wider interval of wind speeds, as can also be seen in the spectra of Fig. 11. Interestingly, the saturation level appears to be slightly lower at the highest wind speeds. This phenomenon may be caused by the high speed winds blowing the tops off of short-wavelength waves and beating them down with spray. Scatter at 2.34 Hz is similar to that observed at 1.41 Hz. At 9.84 Hz, the noise level is fairly constant at the lower wind speeds (the noise floor), and scatter is generally less than 10 dB throughout the plot.

At least three factors may contribute to scatter in these data. The first is simply the error in the measurement due to the randomness of the stochastic processes producing the noise. The chi-squared statistics underlying these spectral measurements lead to a range of scatter of about 3 dB for 90% of the data. This may be all that is needed to explain the scatter in the saturated noise. The second factor is that wind speed is measured at Wake Island, and not directly over the hydrophones. Hydrophone 74, for example, is more than 100 km away from Wake. Thus, there may be a lead time or a lag time or even no correspondence at all between wind speeds at Wake Island and wind speeds directly over the hydrophones. The third factor is that wind wave heights are a function of the duration of the wind and the fetch over which it blows, as well as the wind speed. For example, in the case of a fresh wind blowing over a calm sea, it is well known that long-period wind waves take more time to reach saturation than short-period wind waves. There is supportive evidence for this phenomenon in the correlation lags between the noise and wind

speed time series previously discussed. A delay between the onset of wind and the corresponding onset of noise has also been observed and described by Duennebier *et al.*<sup>36</sup> Thus, scatter is introduced into these plots by the nature of the mechanism that converts wind energy into wave energy, since it seems likely that the noise is caused by the wind waves rather than by the wind.

Note from these plots that the distribution of the 1460 noise levels at each frequency is not Gaussian. Referring back to Fig. 5, the standard deviations shown should be viewed appropriately.

Also note that from the Fig. 12 plots for 1.41 and 2.34 Hz, it might be misconstrued that the saturation level is merely an artifact of plotting noise levels using a logarithmic scale (dB). If noise levels in non-logarithmic units ( $\mu\text{Pa}/\sqrt{\text{Hz}}$ ) are linearly related to wind speed, and the scatter is uniform at all wind speeds, then plots of these data in dB might look similar to the plots in the figure. The data would bend to the right, and the scatter would appear reduced at higher noise levels. However, the WIHA data were tested for this possibility by making such non-logarithmic plots, and the saturation level remained a clear feature of the data.

### VII. CONCLUSIONS

Ambient infrasonic ocean noise levels observed over a period of 1 yr on four hydrophones in the northwestern Pacific near Wake Island vary with wind speed at the ocean's surface at rates of up to 2 dB per m/s. This wind-related noise is categorized into three types. The first type, observed between 0.4 and 6 Hz on two deep-bottom hydrophones and one suspended SOFAR hydrophone, is characterized by levels that rise with wind speed to a clearly defined saturation level—the Holu Spectrum. The data suggest that this noise is directly related to the spectrum of wind waves on the ocean's surface, with a correspondence between saturation of the wind waves and saturation of the noise. The Holu Spectrum has a slope of about  $-23$  dB/octave and a level of about 75 dB relative to  $1 \mu\text{Pa}/\sqrt{\text{Hz}}$  at 4 Hz, and it appears to vary little if at all with depth in the water column. It is probably a worldwide constant. Between 0.3 and 0.8 Hz, the noise has minimum

levels that define a slope of about  $-30$  dB/octave. This slope may be the high-frequency flank of microseism-peak-type noise. The second type of wind-related noise, observed between 4 and 30 Hz on all four hydrophones studied, is characterized by spectral slopes markedly less steep than those observed for the first type of noise, and also by the absence of a saturation level. At higher wind speeds this noise overrides the saturation level of the first type of noise. Wind waves breaking on the sea surface may be the source of this noise. The third type of wind-related noise is observed between about 0.5 and 10 Hz on the SOFAR hydrophone anchored near Wake Island. It is characterized by much higher absolute levels relative to those observed on the other three hydrophones. These higher levels and the close proximity of this hydrophone to Wake Island suggest that this noise is probably generated by wind waves breaking on the shore of the island.

## ACKNOWLEDGMENTS

Appreciation is expressed to Daniel Walker, Eduard Berg, Robert Cessaro, William Prothero, and Thomas Schroeder for their valuable comments and discussions. Firmin Oliveira patiently programmed and ran many of the data collection and processing routines. Kentron Corporation and the U.S. Air Force, Det. 4, 15th ABW provided diligent day-to-day support of the data collection system at Wake Island. Editorial comments and corrections were made by Barbara Jones. Support for this research came from the Office of Naval Research, Code 1125GG, the Air Force Office of Scientific Research (Contract No. F49620-86-C-0003 and Grant No. 86-0039), and the U.S. Arms Control and Disarmament Agency. This work was performed in partial fulfillment of the requirements for the degree of Doctor of Philosophy in geology and geophysics. School of Ocean and Earth Science and Technology 3159.

- <sup>1</sup>M. S. Longuet-Higgins, "A Theory of the Origin of Microseisms," *Philos. Trans. R. Soc. London Ser. A* **243**, 1-35 (1950).
- <sup>2</sup>M. Miche, "Mouvements Ondulatoires de la Mer en Profondeur Constante on Decroissante," *Ann. Ponts Chaussees* **114**, 25-87 (1944).
- <sup>3</sup>K. Hasselmann, "A Statistical Analysis of the Generation of Microseisms," *Rev. Geophys.* **1**, 177-210 (1963).
- <sup>4</sup>R. A. Haubrich, W. H. Munk, and F. E. Snodgrass, "Comparative spectra of microseisms and swell," *Bull. Seismol. Soc. Am.* **53**, 27-37 (1963).
- <sup>5</sup>G. Latham, R. Anderson, and M. Ewing, "Pressure Variations Produced at the Ocean Bottom by Hurricanes," *J. Geophys. Res.* **72**, 5693-5704 (1967).
- <sup>6</sup>G. Latham and A. Nowroozi, "Waves, Weather, and Ocean Bottom Microseisms," *J. Geophys. Res.* **73**, 3945-3956 (1968).
- <sup>7</sup>J. Oliver and M. Ewing, "Microseisms in the 11- to 18-second Period Range," *Bull. Seismol. Soc. Am.* **47**, 111-127 (1962).
- <sup>8</sup>G. M. Wenz, "Acoustic Ambient Noise in the Ocean: Spectra and Sources," *J. Acoust. Soc. Am.* **34**, 1936-1956 (1962).
- <sup>9</sup>N. Barstow, G. H. Sutton, and J. A. Carter, "Particle Motion and Pressure Relationships of Ocean Bottom Noise at 3900 m depth: 0.003 to 5 Hz," *Geophys. Res. Lett.* **16**, 1185-1188 (1989).

- <sup>10</sup>B. R. Kerman, "Underwater Sound Generation by Breaking Wind Waves," *J. Acoust. Soc. Am.* **75**, 149-165 (1984).
- <sup>11</sup>A. C. Kibblewhite and K. C. Ewans "Wave-wave Interactions, Microseisms, and Infrasonic Ambient Noise in the Ocean," *J. Acoust. Soc. Am.* **78**, 981-994 (1985).
- <sup>12</sup>R. H. Nichols, "Infrasonic Ambient Ocean Noise Measurements: Eleuthera," *J. Acoust. Soc. Am.* **69**, 974-981 (1981).
- <sup>13</sup>R. H. Nichols, "Infrasonic Ocean Noise Sources: Wind Versus Waves," *J. Acoust. Soc. Am.* **82**, 1395-1402 (1987).
- <sup>14</sup>A. J. Perrone, "Infrasonic and Low-Frequency Ambient Noise Measurements on the Grand Banks," *J. Acoust. Soc. Am.* **55**, 754-758 (1974).
- <sup>15</sup>G. H. Sutton and N. Barstow, "Ocean-Bottom Ultralow-Frequency (ULF) Seismo-Acoustic Ambient Noise: 0.002 to 0.4 Hz," *J. Acoust. Soc. Am.* **87**, 2005-2012 (1990).
- <sup>16</sup>S. C. Webb and C. S. Cox, "Observations and Modeling of Seafloor Microseisms," *J. Geophys. Res.* **91**, 7343-7358 (1986).
- <sup>17</sup>J. H. Wilson, "Very Low Frequency (VLF) Wind-Generated Noise Produced by Turbulent Pressure Fluctuations in the Atmosphere near the Ocean Surface," *J. Acoust. Soc. Am.* **66**, 1499-1507 (1979).
- <sup>18</sup>C. S. McCreery, "Yield Estimation from Spectral Amplitudes of Direct P and P Coda Recorded by the Wake Island Deep Ocean Hydrophone Array," *Bull. Seismol. Soc. Am.* **77**, 1748-1766 (1987).
- <sup>19</sup>C. S. McCreery, D. A. Walker, and G. H. Sutton, "Spectra of Nuclear Explosions, Earthquakes, and Noise from Wake Island Bottom Hydrophones," *Geophys. Res. Lett.* **10**, 59-62 (1983).
- <sup>20</sup>D. A. Walker, "Deep Ocean Seismology," *Eos* **65**, 2-3 (1984).
- <sup>21</sup>D. A. Walker and C. S. McCreery, "Deep Ocean Seismology: Seismicity of the Northwestern Pacific Basin Interior," *Eos* **69**, 742-743 (1988).
- <sup>22</sup>S. N. Thanos, *OBS Calibration Manual* (Lamont Geological Observatory, Columbia Univ., New York, 1966), p. 23.
- <sup>23</sup>N. Barstow, G. H. Sutton, and J. A. Carter, "Particle Motion and Pressure Relationships of Ocean Bottom Noise: 3900 m Depth; 0.003 to 5 Hz," *Geophys. Res. Lett.* **16**, 1185-1188 (1989).
- <sup>24</sup>"Local Climatological Data, Monthly Summaries for Wake Island, PC," National Climatic Data Center, Asheville, NC.
- <sup>25</sup>R. J. Urlick, *Principles of Underwater Sound* (McGraw-Hill, New York, 1983), p. 423.
- <sup>26</sup>W. A. Watkins, P. Tyack, K. Moore, and J. E. Bird, "The 20-Hz signals of finback whales (*Balaenoptera physalus*)," *J. Acoust. Soc. Am.* **82**, 1901-1912 (1987).
- <sup>27</sup>J. Northrop, W. C. Cummings, and M. F. Morrison, "Underwater 20-Hz Signals Recorded Near Midway Island," *J. Acoust. Soc. Am.* **49**, 1909-1910 (1971).
- <sup>28</sup>H. Bradner, "Probing the sea-bottom sediments with microseismic noise," *J. Geophys. Res.* **68**, 1788-1791 (1963).
- <sup>29</sup>C. Cox, T. Deaton, and S. Webb, "A Deep-sea Differential Pressure Gauge," *J. Atmos. Ocean Technol.* **1**, 237-246 (1984).
- <sup>30</sup>J. Brune and J. Oliver, "The seismic noise of the earth's surface," *Bull. Seismol. Soc. Am.* **49**, 349-353 (1959).
- <sup>31</sup>E. Herrin, "The resolution of seismic instruments used in treaty verification research," *Bull. Seismol. Soc. Am.* **72**, S61-S67 (1982).
- <sup>32</sup>F. K. Duennebie, R. K. Cessaro, and P. Anderson, "Geo-acoustic noise levels in a deep ocean borehole," in *Ocean Seismo-Acoustics*, edited by T. Akal and J. M. Berkson (Plenum, New York, 1986), pp. 743-751.
- <sup>33</sup>A. C. Kibblewhite and C. Y. Wu, "The theoretical description of wave-wave interaction as a noise source in the ocean," *J. Acoust. Soc. Am.* **89**, 2241-2252 (1991).
- <sup>34</sup>O. M. Phillips, *The Dynamics of the Upper Ocean* (Cambridge U.P., Cambridge, England, 1977), p. 113.
- <sup>35</sup>C. S. McCreery and F. K. Duennebie, "The Holu Spectrum: A Worldwide Deep-Ocean Constant, and Indicator of the Ocean Wave Spectrum," *Eos* **69**, 1245 (1988).
- <sup>36</sup>F. K. Duennebie, C. S. McCreery, D. Harris, R. K. Cessaro, C. Fisher, and P. Anderson, "OSS IV: noise levels, signal-to-noise ratios, and noise sources," *Init. Rep. DSDP* **88**, 89-103 (1987).